Models of unsteady convective and conductive heating of double-layer printing materials*

Yaroslav Kolyano[1,†], Bohdan Durnyak[1,†], Taras Sass[1,*,†] and Georgij Petriaszwili[2,†]

[1] Lviv Polytechnic National University, 12 Stepan Bandera St., Lviv, 79013, Ukraine
[2] Warsaw University of Technology, 1 Politechniki Sq, Warszawa, 00-661 Poland

Abstract

In modern printing production, trends aimed at improving barrier and strength characteristics lead to an increasingly wide use of multilayer materials (composites). Each layer in such composites is made of a material with qualitatively different properties and serves its own functional purpose. Many of these materials are subjected to thermal treatment (heating and drying) at various stages of production or operation. The main obstacle to intensive thermal treatment is the occurrence of significant temperature and moisture content gradients, which cause considerable thermal and moisture stresses and deformations. A prerequisite (the first step) for studying thermo-moisture conductivity problems (drying problems) is the study of the corresponding heat conduction problems (heating problems), which enables a more thorough analysis of the relevant industrial drying process. Therefore, this paper presents the corresponding mathematical models and provides graphs of convective and conductive temperature distributions for double-layer composite printing materials, allowing observation of emerging temperature gradients and analysis of their role in these processes. The results of numerical calculations can be recommended for enterprises in the printing industry as well as in other fields of production where thermal treatment is applied.

Keywords

heat transfer; unsteady convective heating; unsteady conductive heating; temperature gradients; composite materials; printing materials; mathematical modeling; thermal treatment.[1]

1. Introduction

A significant number of materials used in printing are multilayer bodies, that is, composites. During their production (at various stages of the manufacturing process) and operation, they are subjected to thermal treatment (heating and drying). Such plane-parallel composites in printing include certain special types of paper (coated paper, map paper), cardboard (layered cardboard consisting of various layers such as cellulose, wood pulp, cardboard), cardboard with a protective film, corrugated cardboard; modern packaging materials (paper–lacquer, paper–foil, paper–polyethylene, aseptic three-layer packaging of cardboard–foil–polyethylene); laminated prints (application of polymer by melt coating or by pressing polymer films); bookbinding covers (cardboard, adhesive layer, cover material); book covers (paper base and polymer coating); the spines of book blocks when attaching the block to the cover; printing plates, and others [8, 9, 10, 11, 15, 18, 6]. The main obstacle to intensive thermal treatment of materials is the occurrence of stresses that lead to deterioration in product quality or even its destruction. The reason for the formation of large temperature and moisture stresses and deformations during the heating of a material is the presence of temperature and moisture content fields with significant gradients of these quantities [4, 6]. An important technological factor in heating various materials is the preservation of their shape during subsequent technological operations. Therefore, the selection of

* AdvAIT-2025: 2nd International Workshop on Advanced Applied Information Technologies: AI & DSS, December 05, 2025, Khmelnytskyi, Ukraine, Zilina, Slovakia
[1,*] Corresponding author.
[†] These authors contributed equally.
yaroslav.y.koliano@lpnu.ua (Y. Kolyano); bohdan.v.durnyak@lpnu.ua (B. Durnyak); taras.s.sass@lpnu.ua (T. Sass); georgij.petriaszwili@pw.edu.pl (G. Petriaszwili)
0009-0003-0518-5593 (Y. Kolyano); 0000-0003-1526-9005 (B. Durnyak); 0009-0001-0326-0612 (T. Sass); 0000-0003-0696-5463 (G. Petriaszwili)

the regime parameters of the heating (drying) process plays an important role in determining the technological mode under specific production conditions. Optimization of heating and drying processes for such materials is an urgent task, the solution of which will make it possible to prevent the destruction or damage of materials, improve the operational properties of finished products, use thermal energy efficiently, and reduce production time [8, 11]. The prerequisite (first step) for solving and studying unsteady problems of heat-and-moisture conductivity (drying problems) for multilayer bodies is the solution of the corresponding unsteady heat conduction problems (heating problems). The creation of new high-quality composites will ensure material savings and reduce the weight and thickness of products.

2. Related works

The number of theoretical and practical studies concerning the convective heating method is considerable and continues to grow, especially in the field of high-speed (jet) convection [11] and combined heating methods (conductive–convective, radiative–convective), which are used when a less intensive technological regime is required [8, 11, 2, 17, 20]. The conductive heating method has been studied to a lesser extent, particularly with regard to printing materials [8]. The radiative (infrared or thermal radiation) heating method has been investigated even less [7, 8, 11, 13]. The study of the advantages of various heating methods contributes to the correct selection of the design and operating parameters of drying equipment and enables further control of these processes. In this regard, for the improvement of thermal treatment technologies, the development of analytical research methods for heating and drying processes based on the theories of heat conduction and heat-and-mass transfer (thermo-moisture conductivity) is considered relevant [4, 6, 14]. With the development of information technologies, new opportunities are emerging for the study of the above-mentioned methods of thermal treatment of materials in the printing industry [1].

3. Methodology and presentation of the main research material

The purpose of this paper is to study, based on the proposed models, the behavior of certain double-layer printing materials (the number of layers may be greater) under convective and conductive heating. The next step in the future is to analyze multilayer (composite) materials with predetermined properties (each layer performing its own function), which are able to withstand permissible thermal loads without losing quality during production and operation. The research will be focused on the manufacturing and use of special types of paper and cardboard, bookbinding covers, packaging materials, decorative printing products, military and fire-resistant equipment [3], building materials considered as two- or multi-layer composites (see [6], [16, 19]).

The mathematical models of unsteady convective and conductive heating of a double-layer plate are developed on the basis of the classical theory of heat conduction proposed by O. V. Lykov [4, 5].

Physical formulation of the convective heat conduction problem. An infinite plate composed of two layers having different thermophysical parameters and thicknesses h_1 and h_2 (i.e., a composite of two layers) is considered (see Fig. 1). The initial temperature of both layers is uniform and equal to t_0. At the initial moment of time $\tau = 0$, this composite is placed in a medium with a temperature t_c. Convective heat exchange occurs between the boundary surfaces and the surrounding medium. At the interface between the layers $z=0$, conditions of ideal thermal contact are assumed. It is required to determine the temperature distribution at an arbitrary point z of the double-layer plate as a function of time τ.

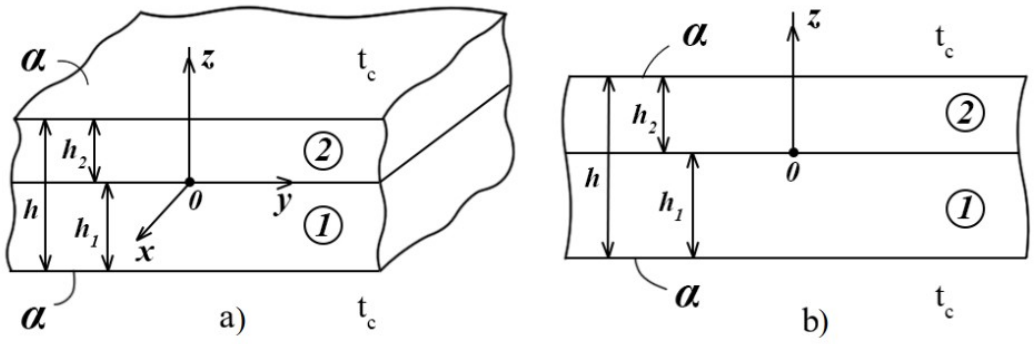

Figure 1: Cross-section scheme of a double-layer plate convectively heated by warm air of temperature t_c: (a) three-dimensional view; (b) two-dimensional view.

The mathematical formulation of the proposed problem can be written as follows:

$$\frac{\partial^2 T_1}{\partial z^2}=\frac{1}{a_1}\frac{\partial T_1}{\partial \tau}, \qquad -h_1<z<0, \qquad \tau>0 \tag{1}$$

$$\frac{\partial^2 T_2}{\partial z^2}=\frac{1}{a_2}\frac{\partial T_2}{\partial \tau}, \qquad 0<z<h_2, \tag{2}$$

$$T_1(z,\tau)=T_2(z,\tau)=0, \qquad \tau=0, \tag{3}$$

$$\lambda_1\frac{\partial T_1}{\partial z}-\alpha(T_1-T_C)=0, \qquad z=-h_1, \tag{4}$$

$$\lambda_2\frac{\partial T_2}{\partial z}+\alpha(T_2-T_C)=0, \qquad z=h_2, \tag{5}$$

$$T_1(z,\tau)=T_2(z,\tau), \qquad \lambda_1\frac{\partial T_1}{\partial z}=\lambda_2\frac{\partial T_2}{\partial z}, \qquad z=0, \tag{6}$$

where $T_1=t_1(z,\tau)-t_0, T_2=t_2(z,\tau)-t_0$ — the sought temperature distributions for the first and second layers of the plate, respectively; $T_c=t_c-t_0$, t_c, t_0 — given quantities; a_j, λ_j — coefficients of thermal diffusivity and thermal conductivity of layers 1 and 2; α — heat transfer coefficient between the plate surfaces and the external environment.

Applying the Laplace transform with respect to time [5, 6] to equations (1)–(6), we obtain:

$$\frac{d^2\overline{T}_j}{dz^2}=\frac{s}{a_j}\overline{T}_j, \qquad \left(j=\overline{1,2}\right) \tag{7}$$

$$\lambda_1\frac{d\overline{T}_1}{dz}-\alpha\left(\overline{T}_1-\frac{T_c}{s}\right)=0, \qquad z=-h_1 \tag{8}$$

$$\lambda_2\frac{d\overline{T}_2}{dz}+\alpha\left(\overline{T}_2-\frac{T_c}{s}\right)=0, \qquad z=h_2 \tag{9}$$

$$\overline{T}_1=\overline{T}_2, \qquad \lambda_1\frac{d\overline{T}_1}{dz}=\lambda_2\frac{d\overline{T}_2}{dz}, \qquad z=0 \tag{10}$$

where s — the Laplace transform parameter; $\overline{T}_j(z,s)$ — Laplace transforms of the temperature functions $T_j(z,\tau)$ in the image space.

The general solutions of the heat conduction equation (7) can be written as:

$$\overline{T}_j(z,s)=A_j ch\, s_j z+B_j sh\, s_j z \ , \qquad (11)$$

where $s_j=\sqrt{\dfrac{s}{a_j}}$ $(j=\overline{1,2})$. The four unknown constants A_1, B_1, A_2, B_2 are determined by substituting solutions (11) into the transformed boundary conditions (8)–(10) and solving the following system of linear algebraic equations:

$$\begin{gathered} A_1=A_2, \qquad K_\varepsilon B_1=B_2 \ , \\ -\delta_{11}A_1+\delta_{12}B_1=-H_1\frac{T_c}{s} \ , \\ \delta_{21}A_1+\delta_{22}B_1=H_2\frac{T_c}{s} \ , \end{gathered} \qquad (12)$$

where $\delta_{11}=s_1 sh\, s_1h_1+H_1 ch\, s_1h_1$, $\delta_{12}=s_1 ch\, s_1h_1+H_1 sh\, s_1h_1$,
$\delta_{21}=s_2 sh\, s_2h_2+H_2 ch\, s_2h_2$, $\delta_{22}=K_\varepsilon\left(s_2 ch\, s_2h_2+H_2 sh\, s_2h_2\right)$,
$K_\varepsilon=\dfrac{K_\lambda}{\sqrt{K_\alpha}}$, $K_\lambda=\dfrac{\lambda_1}{\lambda_2}$, $K_a=\dfrac{a_1}{a_2}$, $H_j=\dfrac{\alpha}{\lambda_j}$ $(j=\overline{1,2})$.

From the system of equations (12), the values of the constants A_1 and B_1 are determined. For convenience, let $H=H_1=\dfrac{\alpha}{\lambda_1}$ $H_2=\dfrac{\alpha}{\lambda_2}=\dfrac{\lambda_1}{\lambda_2}\cdot\dfrac{\alpha}{\lambda_1}=K_\lambda H$. Then, the expressions for the Laplace images of the temperature take the form:

$$\overline{T}_1(z,s)=A_1 ch\, s_1z+B_1 sh\, s_1z=H\frac{T_c}{s}\frac{1}{\psi(s)}\left(\delta_{22}+K_\lambda\delta_{12}\right)ch\, s_1z+$$
$$+H\frac{T_c}{s}\frac{1}{\psi(s)}\left(K_\lambda\delta_{11}-\delta_{21}\right)sh\, s_1z=\frac{T_c}{s}\frac{\Phi_1(z,s)}{\psi(s)}, \qquad (13)$$

$$\overline{T}_2(z,s)=A_2 ch\, s_2z+B_2 sh\, s_2z=H\frac{T_c}{s}\frac{1}{\psi(s)}\left(\delta_{22}+K_\lambda\delta_{12}\right)ch\, s_2z+$$
$$+H\frac{T_c}{s}K_\varepsilon\frac{1}{\psi(s)}\left(K_\lambda\delta_{11}-\delta_{21}\right)sh\, s_2z=\frac{T_c}{s}\frac{\Phi_2(z,s)}{\psi(s)}, \qquad (14)$$

where

$$\Phi_1(z,s)=H\left(\delta_{22}+K_\lambda\delta_{12}\right)ch\, s_1z+H\left(K_\lambda\delta_{11}-\delta_{21}\right)sh\, s_1z,$$
$$\Phi_2(z,s)=H\left(\delta_{22}+K_\lambda\delta_{12}\right)ch\, s_2z+H\,K_\varepsilon\left(K_\lambda\delta_{11}-\delta_{21}\right)sh\, s_2z \ , \quad \psi(s)=\delta_{11}\delta_{22}+\delta_{12}\delta_{21} .$$

To transition from the image space to the original functions, the Vashchenko–Zakharchenko theorem is applied. As a result, the expressions for the temperature distributions in dimensionless form through the criterion parameters are obtained as shown above.

$$T_1^*(Z,Fo)=\frac{T_1(z,\tau)}{T_c}=\frac{2+Bi\left(1+K_hK_\varepsilon\right)}{2+Bi\left(1+\beta K_\varepsilon\right)}+2\,Bi\sum_{n=1}^{\infty}\frac{\Phi_1(Z,\mu_n)}{\mu_n\Psi(\mu_n)}e^{-\mu_n^2Fo}, \quad -1<Z<0 , \qquad (15)$$

$$T_2^*(Z,Fo)=\frac{T_2(z,\tau)}{T_c}=\frac{2+Bi\left(1+K_hK_\varepsilon\right)}{2+Bi\left(1+\beta K_\varepsilon\right)}+2\,Bi\sum_{n=1}^{\infty}\frac{\Phi_2(Z,\mu_n)}{\mu_n\Psi(\mu_n)}e^{-\mu_n^2Fo}, \quad 0<Z<K_h , \qquad (16)$$

where

$$\Phi_1(Z,\mu_n)=A_1(\mu_n)\cos\ \mu_n Z+A_2(\mu_n)\sin\ \mu_n Z\ ,$$
$$\Phi_2(Z,\mu_n)=A_1(\mu_n)\cos(\mu_n\sqrt{K_a}Z)+K_\varepsilon A_2(\mu_n)\sin(\mu_n\sqrt{K_a}Z)\ ,$$
$$A_1(\mu_n)=a_{11}(\mu_n)+a_{12}(\mu_n)\ ,\quad A_2(\mu_n)=a_{21}(\mu_n)-a_{22}(\mu_n),$$
$$a_{11}(\mu_n)=K_\epsilon[\sqrt{K_a}\mu_n\cos(\beta\mu_n)+K_\lambda Bi\sin(\beta\mu_n)]\ ,\ a_{12}(\mu_n)=K_\lambda(\mu_n\cos\mu_n+Bi\sin\mu_n)\ ,$$
$$a_{21}(\mu_n)=K_\lambda(Bi\cos\mu_n-\mu_n\sin\mu_n)\ ,\ a_{22}(\mu_n)=K_\lambda Bi\cos(\beta\mu_n)-\mu_n\sqrt{K_a}\sin(\beta\mu_n),$$
$$\Psi(\mu_n)=b_1(\mu_n)\cos\mu_n\cos(\beta\mu_n)+b_2(\mu_n)\sin\mu_n\sin(\beta\mu_n)-$$
$$-\mu_n b_3(\mu_n)\sin\mu_n\cos(\beta\mu_n)-\mu_n b_4(\mu_n)\cos\mu_n\sin(\beta\mu_n)$$
$$b_1(\mu_n)=2K_\lambda Bi-\beta\sqrt{K_a}\mu_n^2+\beta K_\lambda K_\epsilon Bi^2+\sqrt{K_a}Bi^2-K_\lambda\mu_n^2\ ,$$
$$b_2(\mu_n)=\sqrt{K_a}\mu_n^2+\beta K_\lambda\mu_n^2-Bi\sqrt{K_a}(K_\epsilon^2+1)-K_\lambda K_\epsilon Bi^2-\beta\sqrt{K_a}Bi^2,$$
$$b_3(\mu_n)=2K_\lambda+2K_\lambda Bi+\beta Bi\sqrt{K_a}(K_\epsilon^2+1)\ ,\ b_4(\mu_n)=2\sqrt{K_a}+2\beta Bi K_\lambda+Bi\sqrt{K_a}(K_\epsilon^2+1)$$
$$Bi=\frac{\alpha}{\lambda_1}h_1\ ,\ Z=\frac{z}{h_1},\quad Fo=\frac{a_1\tau}{h_1^2}\ ,\ \beta=K_h\sqrt{K_a}\ ,\ K_h=\frac{h_2}{h_1}\ .$$

The quantities μ_n are the roots of the characteristic equation

$$2K_\epsilon Bi\,\mu\cos\mu\cos(\beta\mu)-Bi\,\mu(K_\epsilon^2+1)\sin\mu\sin(\beta\mu)+$$
$$+(K_\epsilon^2Bi^2-\mu^2)\cos\mu\sin(\beta\mu)+K_\epsilon(Bi^2-\mu^2)\sin\mu\cos(\beta\mu)=0\ .$$

Physical formulation of the conductive heat transfer problem. An infinite plate of total thickness h composed of two layers (see Fig. 2) is considered. The layers have different thermophysical properties and thicknesses h_1 and h_2. The initial temperature of both layers is the same and equal to t_0. At the initial moment of time $\tau=0$, the upper surface z = h, which interacts with the surrounding medium according to the law of convective heat exchange, is exposed to a temperature t_c, while the lower surface z = 0 is heated by a heat flux q. At the interface $z = h_1$, the conditions of perfect thermal contact are assumed. It is required to determine the temperature distribution at an arbitrary point z of this double-layer plate as a function of time τ.

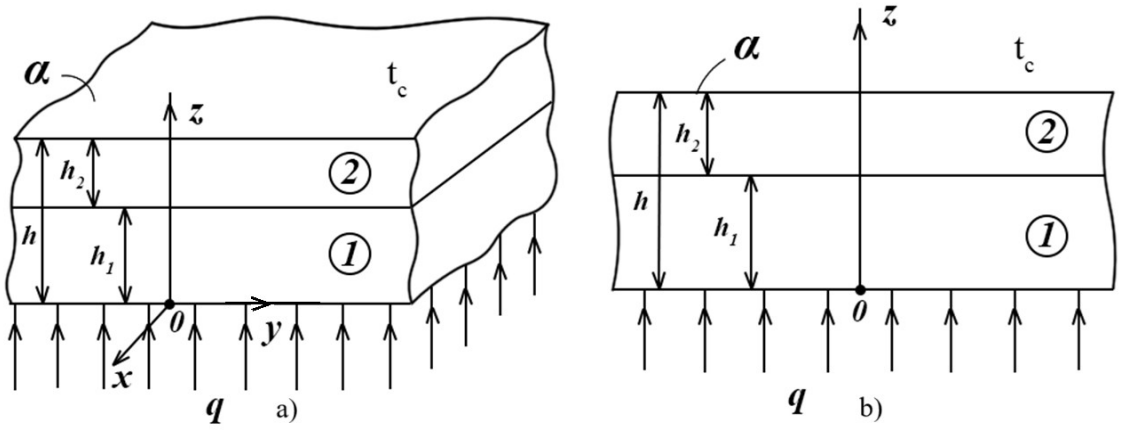

Figure 2: Diagram of a cross-section of a two-layer plate conductively heated by a heat flux q: a) three-dimensional; b) two-dimensional

This problem was solved and analyzed in [6].

4. Numerical experiment and research results

In this study, a numerical comparison between conductive and convective heating of double-layer printing materials is carried out. To determine the behavior of the unsteady temperature field of a double-layer plate under conductive heating, numerical calculations were performed using formulas (7) and (8) from paper [6] in the Fortran programming environment. The numerical

analysis was conducted for a double-layer composite made of polyurethane (first layer) and cardboard (second layer) (see Fig. 3). The choice of these materials is justified by the significant differences in their thermophysical parameters λ and a for polyurethane and cardboard, which make it possible to observe pronounced temperature gradients, especially within the polyurethane layer. If another polymer such as polyethylene or polypropylene is used for the first layer, the temperature gradients in this layer are smaller [5]. The thermophysical parameters are as follows: for polyurethane: $\lambda_1=0.026\frac{W}{(m\,^\circ C)}$, $a_1=0.3\times10^{-6}\frac{m^2}{s}$ [6]; for cardboard: $\lambda_2=0.2\frac{W}{(m\,^\circ C)}$, $a_2=0.174\times10^{-6}\frac{m^2}{s}$, $\alpha\approx11.7\frac{W}{(m^2\,^\circ C)}$[6]; $t_0=10\,^\circ C$, $t_c=30\,^\circ C$, $q=1000\frac{W}{m^2}$. These input temperature parameters correspond to the production and experimental values given in [3, 5, 6, 11, 12].

Using formulas (7) and (8) from [6], the temperature distributions over time were calculated for the double-layer polyurethane–cardboard (composite) plates with total thicknesses of 10 mm (1 mm + 9 mm) and 2 mm (1 mm + 1 mm) under conditions of conductive heating (see Fig. 3). In both cases, the temperature reaches its maximum value at the end of the heating process (i.e., when the plate is fully heated through). Temperature gradients (differences across the plate thickness) appear from the initial time moments and reach their maximum at the end of heating. Polyurethane is a significantly better thermal insulator than cardboard (it retains heat more effectively), therefore, the temperature gradients that occur within it are much higher than in cardboard (see Fig. 3b, 3d). As the plate thickness increases, the magnitude of the temperature gradient between its surfaces also increases (see Fig. 3b, 3d). When these gradients reach critical values, they generate dangerous stresses and deformations that lead to material failure (delamination or cracking). Such stresses and deformations are particularly hazardous along the interface between the layers $z=h_1$ due to the considerable difference in their thermophysical parameters. The heating duration under a heat flux $q=1000\frac{W}{m^2}$ can be evaluated from the secondary time axes for the real time τ (see Fig. 3a, 3c): for the 10 mm plate, heating lasts about 1 hour; for the 2 mm plate — about 0.1 hour (6 minutes). Furthermore, the unsteady temperature graphs in Fig. 3 make it possible to observe the maximum (including critical) temperature values that occur in the composite during heating. For instance, under heating by a heat flux $q=1000\frac{W}{m^2}$, the polyurethane–cardboard composite plate of 10 mm thickness reaches a surface $z=0$ temperature of $t_{max}\approx190\,^\circ C$ (see Fig. 3a). For polyurethane, this value represents the critical temperature at which melting begins.

The numerical solution of the unsteady heat conduction problem for the double-layer polyurethane–cardboard plates with total thicknesses of 10 mm (1 mm + 9 mm) and 2 mm (1 mm + 1 mm) under convective heating (see Fig. 4) was performed using formulas (15) and (16). A computational module was developed in Fortran to calculate the unsteady temperature distribution for t_0 = 10°C and t_e = 80 °C. From the obtained graphs, the time-dependent behavior of the temperature at different points in the plate can be observed, as well as its transition to a steady-state value and the magnitude of the temperature gradients over time (see Fig. 4).

The largest temperature differences across the plate thickness (temperature gradients) appear from the initial moments of heating. This characteristic distinguishes the convective problem from the previous conductive one, where the maximum gradients occurred near the end of the heating process (see Fig. 3b, 3d). The temperature gradients persist until τ ≈ 0.645 h (38.7 min) for the 10 mm plate and τ ≈ 0.0645 h (3.87 min) for the 2 mm plate (see Fig. 4a, 4c). Since polyurethane is a better thermal insulator than cardboard (it retains heat more efficiently), the temperature differences within it are greater. With increasing plate thickness, the temperature gradient between the plate surfaces increases (see Fig. 4b, 4d). When these gradients reach critical values, they generate dangerous stresses and deformations that can lead to composite damage (delamination or

cracking). The greatest deformation risk occurs along the interface between the layers $z=0$ due to the large difference in thermophysical parameters. The total heating duration for the 10 mm plate is approximately 0.74 h (44.4 min), and for the 2 mm plate — about 0.074 h (4.44 min) (see Fig. 4a, 4c). Analyzing the results, it can be concluded that the convective heating method is safer ("softer") for the materials under consideration compared to the conductive one, as the magnitude of the resulting temperature gradients is significantly smaller.

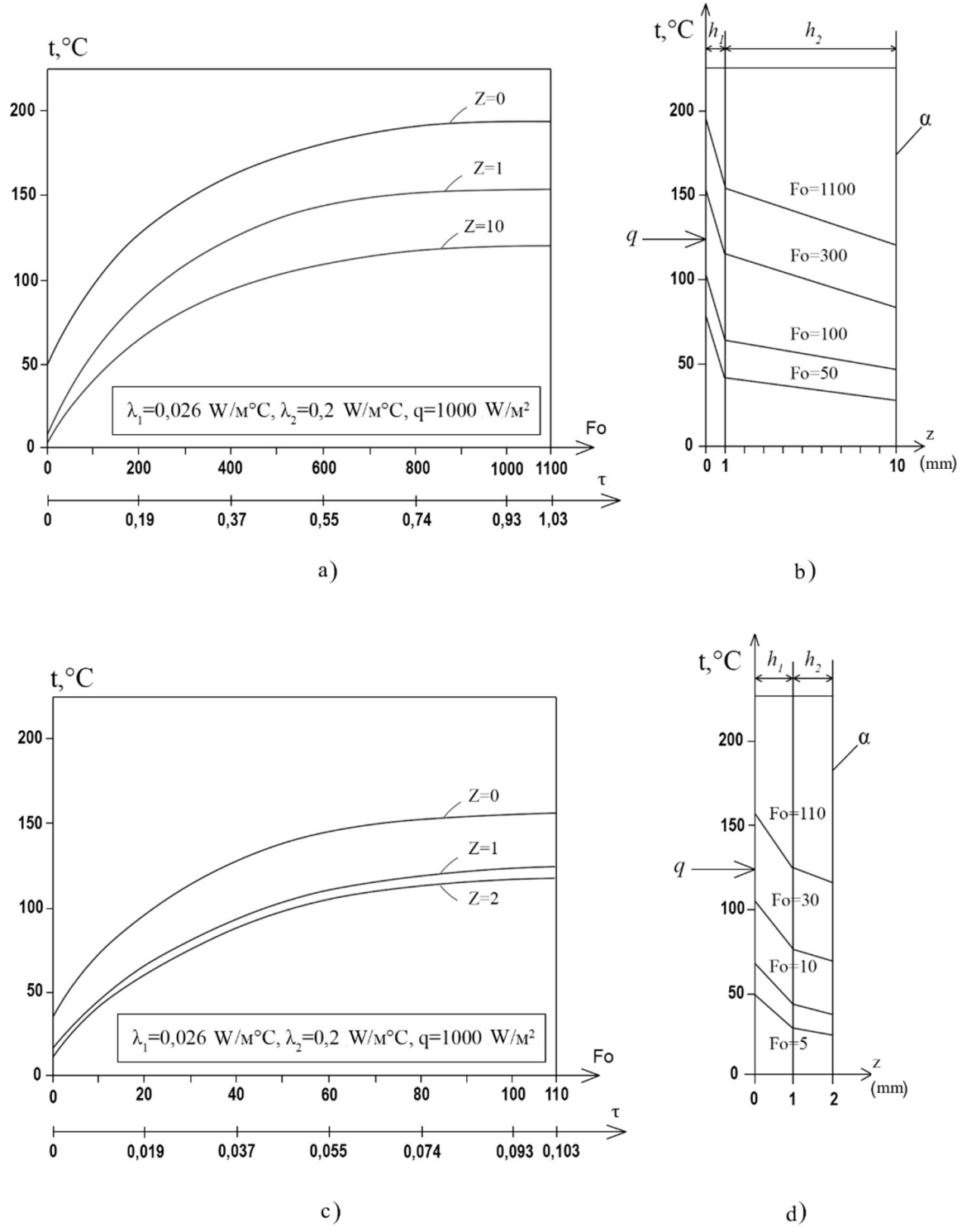

Figure 3: Unsteady temperature distributions over time during conductive heating by heat flux q of a double-layer plate made of polyurethane and cardboard with a total thickness of 10 mm (1 mm + 9 mm) and 2 mm (1 mm + 1 mm):

(a), (c) – as functions of time; (b), (d) – across the plate thickness.

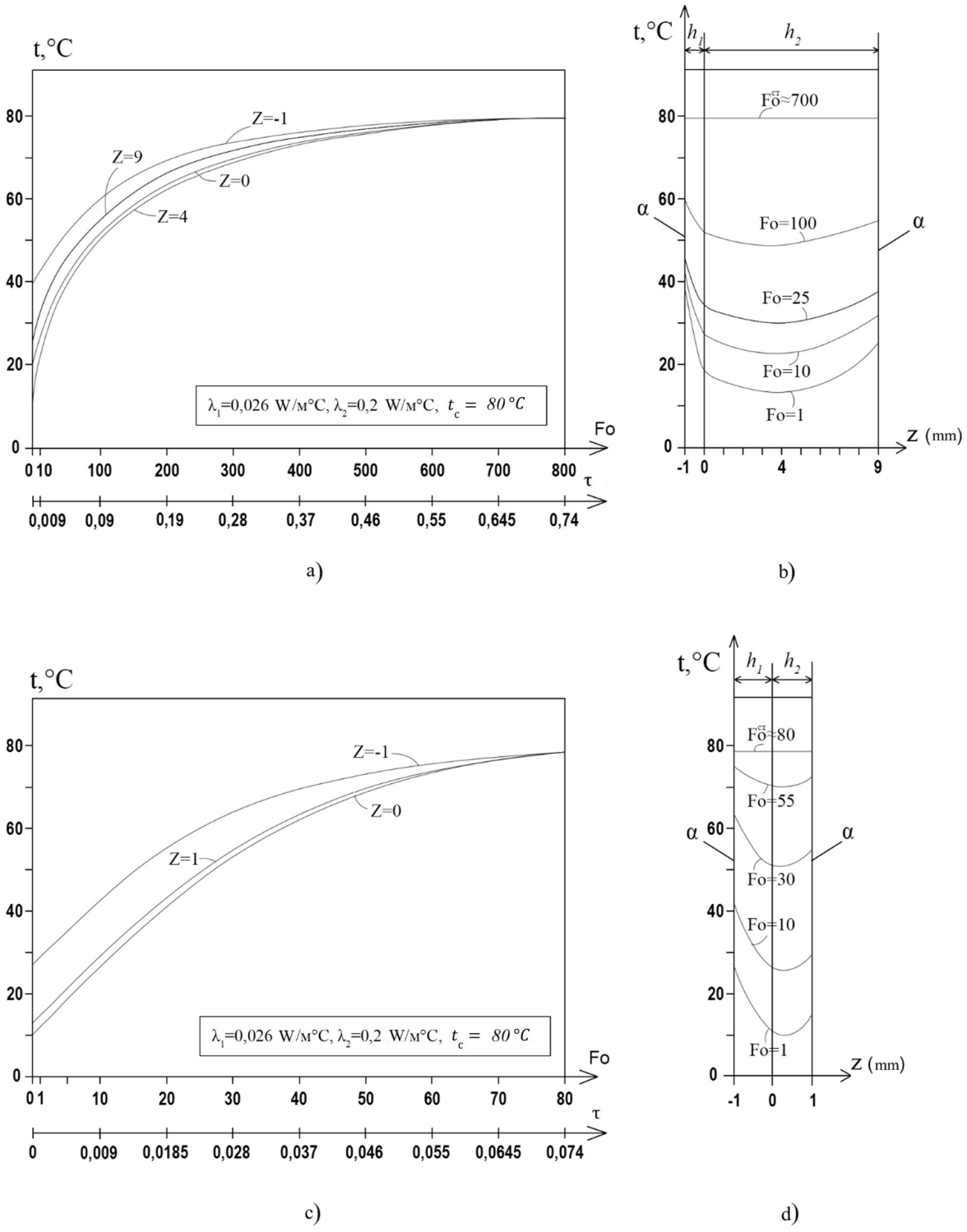

Figure 4: Unsteady temperature distributions over time during convective heating at temperature t_e of a double-layer plate made of polyurethane and cardboard with a total thickness of 10 mm (1 mm + 9 mm) and 2 mm (1 mm + 1 mm):

(a), (c) – as functions of time; (b), (d) – across the plate thickness.

5. Conclusions

Using the developed mathematical models of unsteady convective and conductive heating of double-layer plates and the corresponding software modules, temperature–time behavior graphs were constructed for the polyurethane–cardboard composite. The considered models are useful for studying the thermal treatment processes (heating and drying) of printing materials over time, where heat is supplied by convective or conductive means. These processes are relevant to the production and use of various types of cardboard, paper, textile materials, book covers, packaging materials, and decorative finishing of printing products (for example, polymer film lamination).

A comparison of numerical results for the unsteady convective and unsteady conductive problems shows that the temperature field behavior over time differs significantly between the two heating modes. The dynamics of the process on the unsteady temperature graphs are observed during the transient time moments (i.e., before the plate is fully heated). Hazardous temperature gradients in conductive heating occur at the end of the process, whereas in convective heating they appear at the beginning.

The obtained temperature profiles demonstrate that, for both convective and conductive heating, increasing material thickness leads to larger temperature gradients between the plate surfaces. These gradients generate thermal stresses and deformations that can cause material damage. The most hazardous gradients (and resulting stresses and deformations) occur at the interface between layers due to significant differences in their thermophysical properties. The thicker the plate, the longer the time required to reach steady-state temperature conditions, i.e., the plate heats up longer.

Numerical calculations confirm that the smaller the value of the thermal conductivity coefficient λ, the better the material retains heat, meaning it acts as a more effective thermal insulator. Thus, based on the λ value, a process engineer can determine whether a plate made from a given material behaves as a thermal insulator.

Mathematical modeling of heating processes and analysis of various heating methods for the studied materials enable the design of new composite materials with predefined thermophysical properties. The developed models and their analysis allow determining the optimal heating regime, which positively influences material quality and operational characteristics. The created software tools visualize temperature gradients and the time required to reach steady-state conditions (plate full heating time). Selecting suitable material combinations for the composite can reduce its overall thickness and weight without compromising product quality parameters.

Declaration on Generative AI

The authors have not employed any Generative AI tools.

References

[1] J. Zhang, H. Cui, A. L. Yang, F. Gu, C. Shi, W. Zhang, S. Niu, An intelligent digital twin system for paper manufacturing in the paper industry, Expert Systems with Applications, 230 (2023) 120614.

[2] N. Gómez, P. Vergara, Ú. Fillat, J. C. Villar, Effect of metering systems and drying methods on the barrier properties of paper coated with multiple layers of cellulose nanofibres, Prog. Org. Coat., 189 (2024) 108323.

[3] A. I. Olshanskii, *Regular Thermal Regime of Heating of Moist Flat Capillary-Porous Materials during Drying Process*, *J. Eng. Phys. Thermophys.*, 87(6) (2014) 1308–1318.

[4] Y. Y. Kolyano, T. S. Sass, E. G. Ivanik, *Modeling of Conductive Drying of Printing Materials of Capillary-Porous Colloidal Structure*, *J. Eng. Phys. Thermophys.*, 91(5) (2018) 1164–1174.

[5] Y. Y. Kolyano, V. M. Senkivskyi, O. R. Marchuk (Svyryd), K. I. Melnyk, *Numerical Comparison of Unsteady Convective and Conductive Heating of Single-Layer Printing Materials*, *Printing and Publishing Industry*, 2(80) (2020) 81–99.
[6] Y. Y. Kolyano, V. M. Senkivskyi, K. I. Melnyk, M. M. Klyuch, *Study of Conductive Heating of Double- and Triple-Layer Printing Materials*, *Printing and Publishing Industry*, 2(84) (2022) 83–95.
[7] X. Zhou, "Infrared drying of polymer coatings: Heat transfer analysis," Progress in Organic Coatings, vol. 150, 105990, 2021.
[8] R. I. Shot, I. T. Strepko, *Thermal Processes in Printing: Textbook*, Lviv: UAD “Fenix”, 1998, 202 p.
[9] H. Kipphan (Ed.), *Handbook of Print Media: Technologies and Production Methods*, Springer, Berlin, 2001, 1207 p.
[10] G. A. Smook, *Handbook for Pulp & Paper Technologists*, 4th ed., TAPPI Press, Atlanta (USA), 2016, 438 p.
[11] A. S. Mujumdar (Ed.), *Handbook of Industrial Drying*, 4th ed., CRC Press, Boca Raton (USA), 2015, 1333 p.
[12] E. Martín, I. Viéitez, F. Varas, A predictive model for the industrial air-impingement drying of resin impregnated paper, Applied Thermal Engineering, 199 (2021) 117602.
[13] P. Davari, A. Taghian Dinani, H. Nabizadeh, Comprehensive modeling of far-infrared drying process for a combined far-infrared dryer, Discover Food, 4 (2024) 87.
[14] S. J. Kowalski, Intensification of drying processes due to ultrasound enhancement, Chem. Process Eng., 39(3) (2018) 251–262.
[15] D. Meier, J. Messer, T. Slawik, T. Lex, H. Klein, S. Rehfeldt, Investigation and modeling of paper drying in digital-printing, Appl. Therm. Eng., 269 (2025) 125766.
[16] Z. W. Huang, H. L. Dai, Y. C. Wei, Z. W. Sun, Unsteady heat transfer in a multilayer composite cylinder containing porous media, Appl. Therm. Eng., 211 (2022) 118425.
[17] P. Salagnac, P. Glouannec, D. Lecharpentier, Numerical modeling of heat and mass transfer in porous medium during combined hot air, infrared and microwaves drying, Int. J. Heat Mass Transfer, 47(19–20) (2004) 4479–4489.
[18] K. Kinnunen-Raudaskoski, T. Hjelt, U. Forsström, P. Sadocco, J. Paltakari, Novel thin functional coatings for paper by foam coating, TAPPI J., 16(4) (2017) 179–186.
[19] V. Yatskiv, V. Bodnarovskyi, Research of methods of energy efficiency management in buildings based on IoT, Comput. Syst. Inf. Technol., (2) (2022) 42–46.
[20] M. E. Asar, Z. Noori, J. Yagoobi, Numerical investigation of the effect of ultrasound on paper drying, TAPPI J., 21(3) (2022) 127–140.